

*Article*

## Basic Study on Detection of Deteriorated RC Structures Using Infrared Thermography Camera

Fumio Yamazaki<sup>1,a,\*</sup>, Hideomi Ueda<sup>2</sup>, and Wen Liu<sup>1,b</sup>

<sup>1</sup> Department of Urban Environment Systems, Chiba University, Chiba 263-8522, Japan

<sup>2</sup> Engineering Division, Kajima Corporation, Tokyo 107-8388, Japan

E-mail: <sup>a</sup>fumio.yamazaki@faculty.chiba-u.jp (Corresponding author), <sup>b</sup>wen.liu@chiba-u.jp

**Abstract.** Infrastructures in the world get old in several decades of their service time. Falling-offs of parts of deteriorated structures were often reported and sometimes caused casualties in Japan and many other countries. When an earthquake occurs, in particular, deteriorated structures have higher possibility to be damaged or collapsed. Thus assessing the health condition of structures is one of the important topics in civil engineering. Considering a large number of structures that have been in service more than 40 years in Japan, efficient evaluation methods are requested. In this regard, non-destructive tests have high possibility to be applied to various structures without affecting their functions. Accordingly, this study focuses on the use of infrared thermography to detect internal deterioration of concrete structures. As a first step of investigation, thermography diagnosis, hammer sounding test and Schmidt rebound hammer test were carried out to detect internal deterioration of a concrete retaining wall located in the campus of Chiba University, Chiba, Japan, and the results were compared to evaluate the capability and accuracy of these diagnosis methods.

**Keywords:** Infrared thermography, hammer sounding test, Schmidt hammer, infrastructure, deterioration.

**ENGINEERING JOURNAL** Volume 22 Issue 3

Received 12 January 2018

Accepted 13 February 2018

Published 28 June 2018

Online at <http://www.engj.org/>

DOI:10.4186/ej.2018.22.3.233

This article is based on the presentation at *The International Symposium of the 11<sup>th</sup> SSMS and the 5<sup>th</sup> RCND 2017* in Bangkok, Thailand, 20<sup>th</sup>-21<sup>st</sup> September 2017.

## 1. Introduction

Modern societies are highly dependent on infrastructures. But infrastructures in the world get old in several decades of their service time and hence, their retrofits and reinforcements become more and more important, especially for developed countries where a large portion of infrastructures were built earlier than a half century ago [1-3]. Concrete flaking of deteriorated tunnels [4] and building walls were often reported and sometimes caused casualties in Japan and many other countries. When an earthquake occurs, deteriorated structures, in particular, have higher possibility to be damaged or to collapse [5]. In addition, safety/damage assessment of buildings [6, 7] and bridges [8, 9] just after the occurrence of an earthquake is important for emergency operations and recovery activities [10]. However, considering a large number of structures in the affected area, efficient on-site damage assessment methods are requested.

Various non-destructive diagnosis methods, which are considered to be more efficient and economical than destructive diagnoses, have appeared in the field of civil engineering and construction [11]. Although they draw significant attention in these days and a number of researches have been carried out, their proper procedures and applicability should be examined more until there are used efficiently to evaluate deterioration of structures. As a non-destructive testing technique, sounding tests by striking with a hammer are often used for the deterioration diagnosis of structures, such as interior walls of tunnels. However, this method takes a long time to apply for long-extended structures, and requires scaffolding for objects in high places. Visual inspection [12] is another common and traditional method for structural health monitoring but it needs experienced technicians/engineers. To overcome these problems, various types of sensors have also been used for structural health monitoring [13]. But the most of health monitoring methods need pre-attached sensors to structures.

Image sensing methods, however, are free from this constraint. Using ordinary visible images (photos), various image processing techniques have been proposed and employed in detecting surface cracks of concrete walls [14, 15], but they cannot identify internal defects. In this regard, infrared thermography [16] has been used recently to detect internal deterioration of concrete structures. This method uses thermal behavior of an object's surface for detecting deteriorated parts from temperature change in time and its spatial variation. In recent years, infrared thermography is frequently used in Japan but there still remain problems. Heating is essential in this method, and hence if the solar energy is used as a source of heating, the method depends on the daytime weather and temperature. Otherwise this method requires a heat source and the possibility of uneven heating may lead to wrong diagnosis. To remedy this problems, several studies have been carried out that combine multiple non-destructive methods for the detection of subsurface deterioration [16, 17] and investigate thermal behavior with active heating and passive heating [18, 19]. Infrared thermography cameras are often used in such studies.

In this study, an infrared thermography diagnosis is carried out to detect internal deterioration of a concrete retaining wall, and the results are compared with those from sounding tests and Schmidt rebound hammer tests [11]. The objective of this study is to examine whether infrared thermography can accurately detect deteriorated parts of concrete structures.

## 2. Test site, Methods and Tools of Deterioration Detection

Infrared thermography tests for deteriorated structures were conducted in the Nishi-Chiba campus of Chiba University, Chiba Prefecture, Japan (Fig. 1). There were several concrete surfaces which might be suffered from deterioration. Among them, an existing reinforced-concrete (RC) retaining wall shown in Fig. 1(c) was selected as a target object since this wall was seen apparently to be deteriorated, and located at an easy-to-access place. This retaining wall was built in 1962 as a part of boundary fence, which separates Chiba University's campus and the experiment station of the University of Tokyo. The wall is faced to the west and the sun light illuminates it in the afternoon, which provides uniform heating to the wall.

The observation of the RC retaining wall was carried out using an infrared thermography camera InfReC R300SR-S (Nippon Avionics co, ltd. [20]) as shown in Fig. 2(a, b). The camera has the frame rate of 60 Hz, measuring range from  $-40^{\circ}\text{C}$  to  $120^{\circ}\text{C}$ , and sensitivity  $0.025^{\circ}\text{C}$ . The mechanism to detect deterioration of concrete by infrared thermography is shown in Fig. 2(c). If there is a void part near the surface of concrete, its surface temperature increases more rapidly than a healthy part does under the solar illumination because heat transfer by conduction is hindered by the void. Due to the trapped heat, the surface temperature above the void will increase under a heating condition.

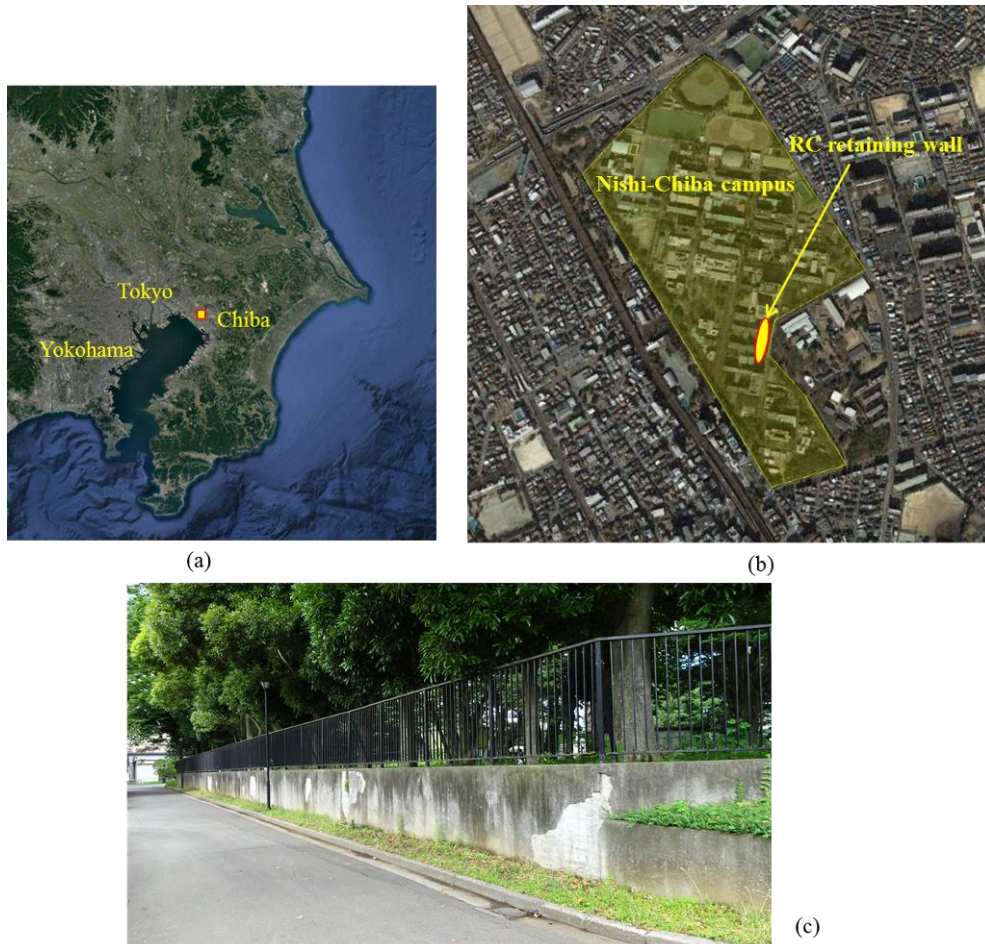


Fig. 1. (a) Location of Chiba City, Japan on Google Earth, (b) Nishi-Chiba campus of Chiba University, and (c) RC retaining wall used in this study.

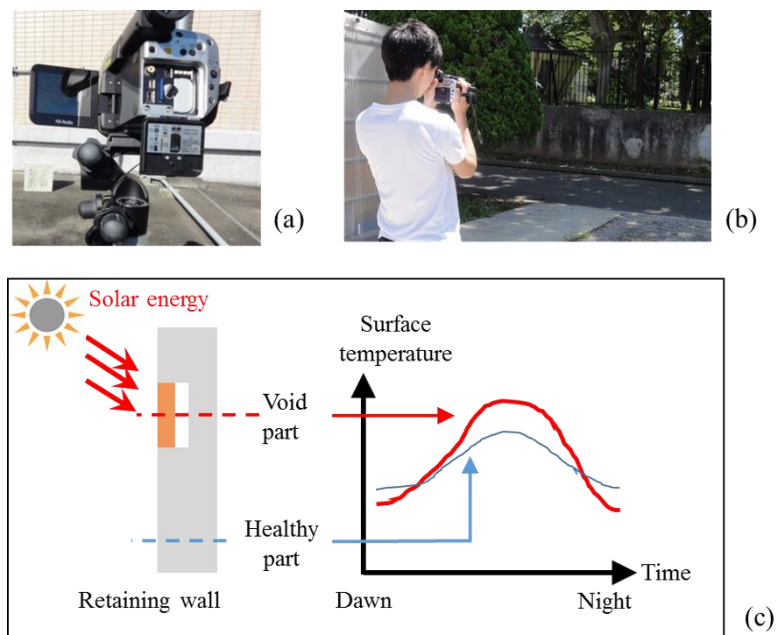


Fig. 2. (a) Infrared thermography camera InfReC R300SR-S, (b) a scene of observation, (c) schematic image of surface temperature change of concrete wall.

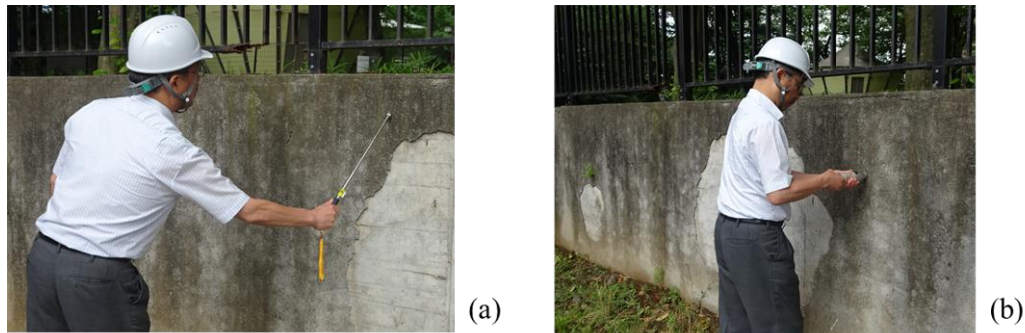


Fig. 3. (a) Scenes of rotary hammering sound test and (b) Schmidt rebound hammer test.

In the thermography diagnosis, the surface temperature was observed by the thermography camera, which evaluates deterioration parts from the temporal change and spatial distribution of temperature. A rotary hammering sound tester [21, 22], shown in Fig. 3(a), was also used for the deteriorated parts that were detected by infrared thermography and their neighboring areas. When the rotary hammer knocked the concrete retaining wall, the sound was recorded by a digital voice recorder and the data were analyzed to characterize deteriorated parts. Additionally, the compressive strength of concrete was also measured by a Schmidt rebound hammer type-N [23, 24] shown in Fig. 3(b). The concrete compressive strength,  $F_c$  ( $\text{N}/\text{mm}^2$ ), can be estimated by the following formula [24]:

$$F_c = \alpha_n [1.27(R_0 + R_1 + R_2) - 18.0] \quad (1)$$

where  $\alpha_n$  is the correction of the concrete age,  $R_0$  is the rebound value measured by the Schmidt hammer,  $R_1$  is the correction coefficient of moisture condition, and  $R_2$  is the correction of the knocking angle.

### 3. Visual Inspection and Measurements of the Retaining Wall

Observation of the RC retaining wall was carried out from 11:00 to 19:30 on July 8, 2014. The weather was sunny with the maximum temperature  $32^\circ\text{C}$  and minimum temperature  $21^\circ\text{C}$ . The sun light illuminated the wall from about 12:30 until about 18:00. These conditions were suitable for infrared thermography. The surface temperature of the RC wall was observed every 30 minutes by the infrared thermography camera. Before starting the tests, the target retaining wall was inspected visually as shown in Fig. 4. It is clearly observed that the cover mortar of the retaining wall had been deteriorated and fall-off holes of mortar were observed at several locations. Deep cracks were also developed to the surface and body of the wall. The existence of voids underneath the cover mortar was also suspected at some locations but it was not so obvious by visual inspection.

Figure 5(a) shows the photograph of the concrete retaining wall including three areas (the blue dotted square in Fig. 4) that were chosen for calculating the mean values of temperature and the temperature change in time (Fig. 5(b)). From this figure, the amount of temperature rise was large in the order of the areas B, A and C. In the area B, in addition to the highest temperature rise, the surface temperature dropped sharply after the sunset. If the wall has internal voids, the heat transfer is blocked by the voids and the heat is likely to accumulate in the surface layer. Accordingly, the temperature increases sharply in the heating time. In the cooling time, the heat in the surface layer is lost in a short time and thus the temperature decreases sharply. Based on this reason and the temperature change in each area, there was high possibility that the areas B and A had internal voids.

Figure 6 shows the distribution of surface temperature at two time instants, 15:30 and 19:30. The surface temperature shows clear difference at the three locations. At the area C, the solid concrete body was exposed and hence a long time was needed until its surface temperature went up. Thus in the stage of heating (15:30), the solid parts, like the area C, have much lower temperature than other parts. On the contrary, the surface temperature went up much faster at suspected deteriorated parts, such as B and A, in the heating stage. But when the heating stopped and the air temperature went down (19:30), the reverse phenomenon was observed. Heat was lost from the deteriorated parts faster than that of the solid part and the surface temperature of the solid part was kept higher than that of the deteriorated parts.

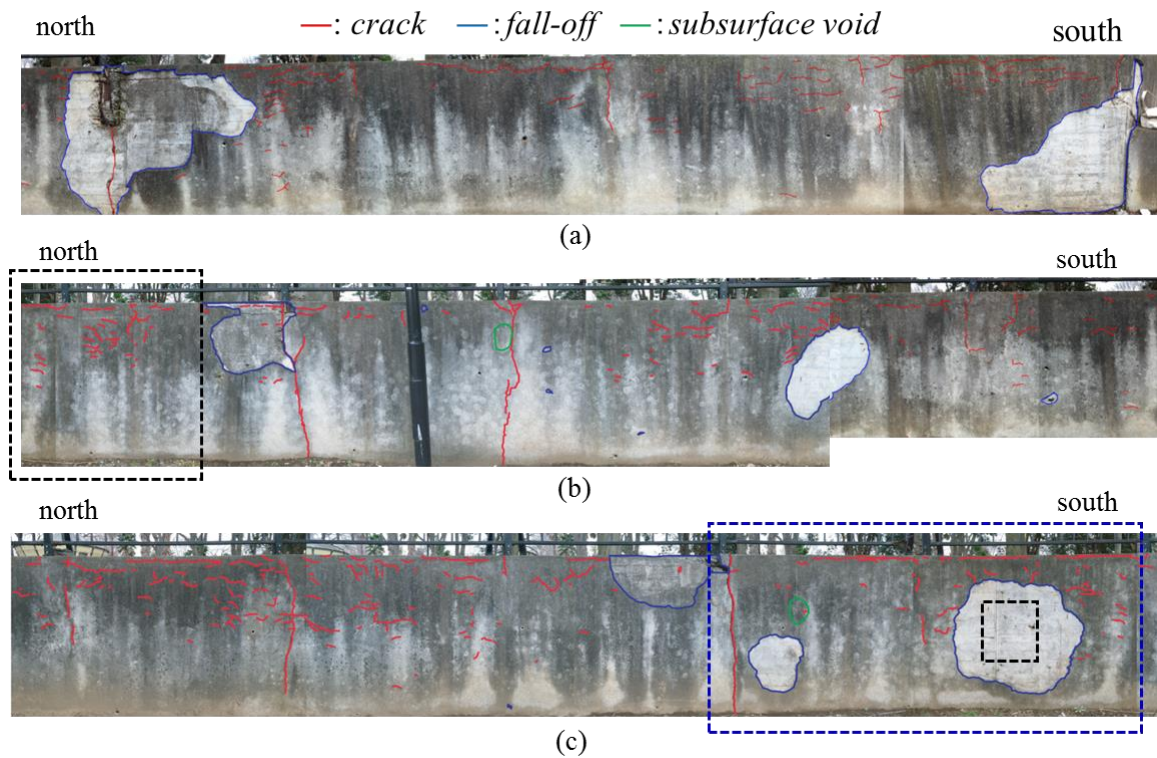


Fig. 4. Photograph of the west surface of the RC retaining wall. The order of (a), (b), and (c) from the south to the north. Deterioration stage was visually inspected and the results were plotted by red line (crack), blue line (flaking hole), and green line (suspected subsurface void). Blue dotted line shows the primary survey area and black dotted line is the Schmidt hammer test area.

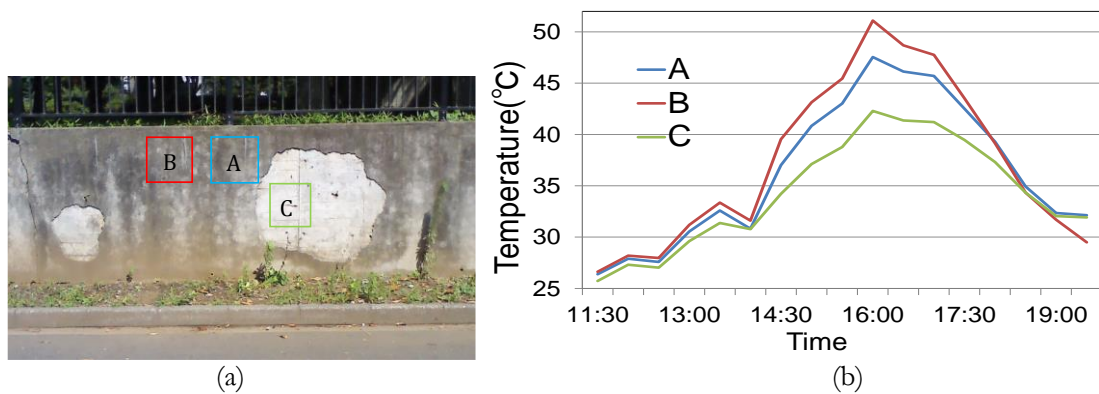


Fig. 5. (a) Location of three typical parts of the measurement area on the retaining wall and (b) the change of temperature in time at these parts on July 8, 2014.

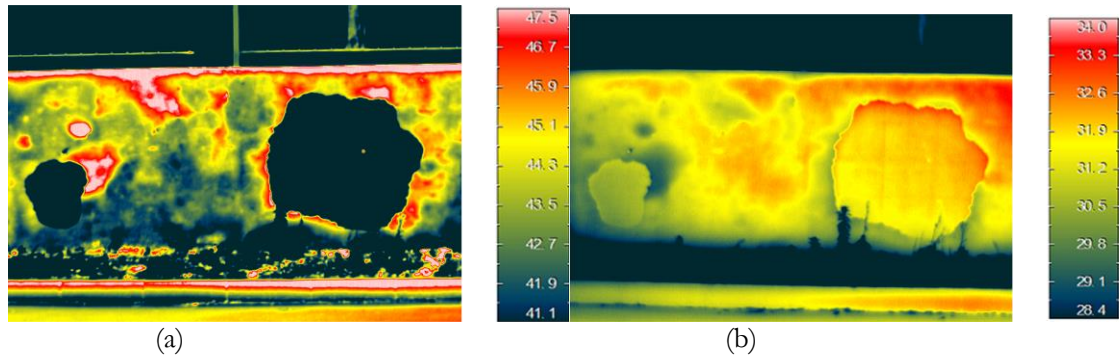


Fig. 6. (a) The surface temperature at 15:30 and (b) 19:30 on July 8, 2014, observed by the infrared thermography camera.

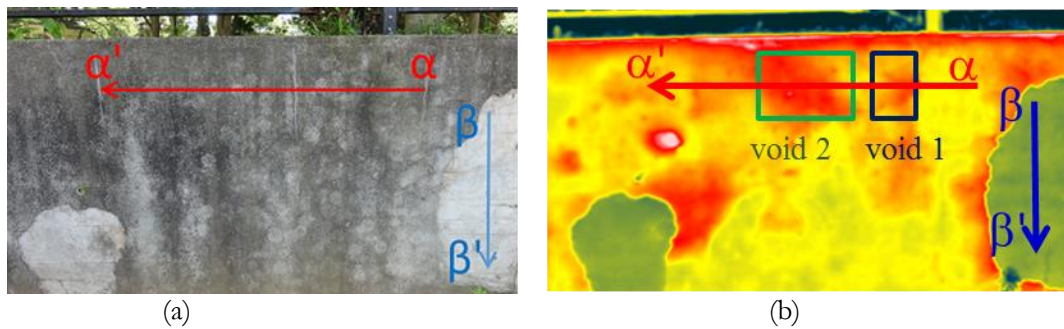


Fig. 7. (a) Measurement area of rotary hammering test (lines  $\alpha$ - $\alpha'$  and  $\beta$ - $\beta'$ ) and (b) thermal images at 15:30, July 8, 2014.

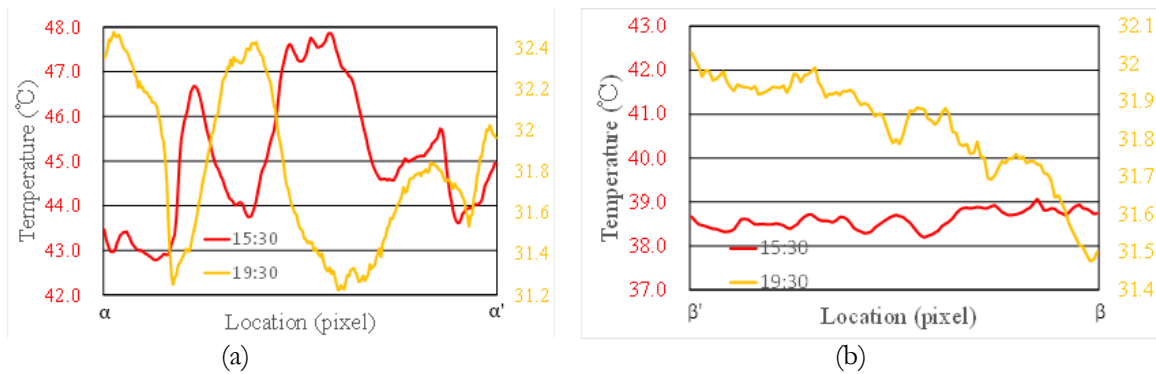


Fig. 8. Distribution of surface temperature at 15:30 (red line) and 19:30 (orange line) on July 8, 2014 along (a) line  $\alpha$ - $\alpha'$  and (b) line  $\beta$ - $\beta'$ .

The temperature distributions suggest us the location of voids underneath the surface mortar. The position and extent of deterioration could be clearly detected using the thermal infrared images. Hence, thermography is considered to be useful in investigating deterioration of large concrete structures at once in a short time. Since the temperature change is different depending on the deterioration state, thermal imagery is effective for assessing the progress of deterioration. But it should be noted that the heating condition affects the change of surface temperature and its spatial distribution.

The deterioration condition of the target area (Fig. 5(a)) was examined in more detail along two lines shown in Fig 7(a). From the thermal images, the line  $\alpha$ - $\alpha'$  was selected in the area of suspected deterioration and the line  $\beta$ - $\beta'$  in the area of peeled-off but no internal deterioration. Figure 8 shows the distribution of surface temperature at 15:30 and 19:30 on July 9, 2014 along the two lines. From the figure, it is clearly seen that the suspected deteriorated part with void shows a higher temperature that that of the solid part in the

heating condition. It is particularly interesting that the trend of temperature along the deteriorated part in the heating time and cooling time was just the opposite.

The deterioration state of the concrete retaining wall was also investigated with the rotary hammer in the area that is shown in Fig. 7. The recorded sound time-histories, the results of time-frequency analysis [25], and the Fourier spectra are plotted in Figs. 9 and 10, respectively for the lines  $\alpha$ - $\alpha'$  and  $\beta$ - $\beta'$ . In the time-frequency plots, the dark color indicates large sound-pressure parts. From the sound-pressure Fourier spectra, the line  $\alpha$ - $\alpha'$  (Fig. 9(c)) has both low-frequency and high-frequency contents but the line  $\beta$ - $\beta'$  has low-frequency contents only (Fig. 10(c)). In addition, the areas that were suspected to be deteriorated by time-frequency analysis (Fig. 9(b)) match the estimated deterioration areas by the thermal image (Fig. 7(b)), in which the deterioration areas exhibited significantly higher temperature. This observation from the rotary hammering test provides a further validation of the usefulness of infrared thermography.

From these verification results, it was found that the rotary hammering test is more efficient than traditional hammering tests. However, the detection of the extent of deterioration and its shape is more difficult than that from thermal imagery. Hammering test cannot assess the deterioration area of large extent at one time. It is also pointed out that a video camera is needed in order to match the knocking area with the amplitudes by the time-frequency sound analysis.

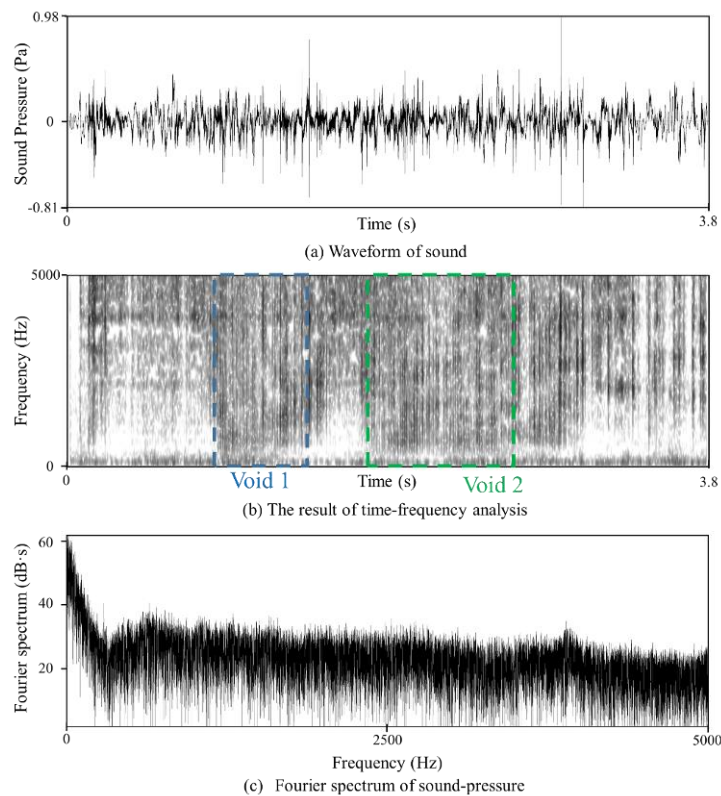


Fig. 9. (a) Recorded sound time-history, (b) its running spectrum, and (c) Fourier spectrum by rotary hammer along the line  $\alpha$ - $\alpha'$  on the retaining wall.

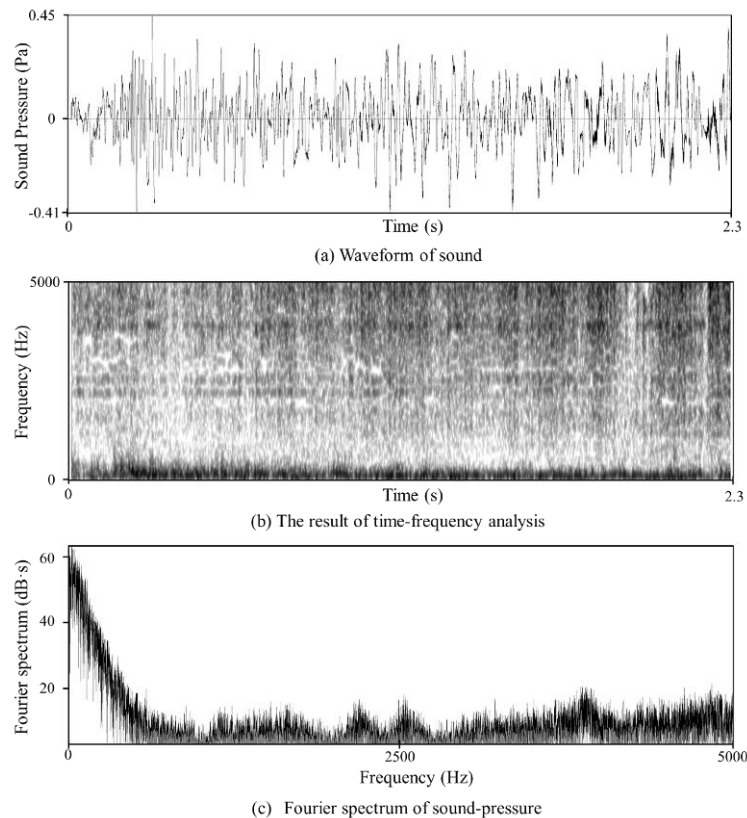


Fig. 10. (a) Recorded sound time-history, (b) its running spectrum, and (c) Fourier spectrum by rotary hammer along the line $\beta$ - $\beta'$  on the retaining wall.

Measurement of the concrete retaining wall by the Schmidt rebound hammer was carried out on June 27, 2013. Three areas measured by Schmidt hammer are illustrated in Fig. 11 and Fig. 4 (dotted black squares). From the thermal image, the area A' was considered to have internal voids, the area B' to be sound and the area C' was already peeled-off and the sound concrete was exposed. In the area A', the rebound value  $R$  was 24.46 and therefore the compressive strength  $F_C$  was calculated by Eq. (1) as 7.87 N/mm<sup>2</sup>. In the area B', the rebound value  $R$  was 28.24 with  $F_C$  10.76 N/mm<sup>2</sup>. The compressive strength of the area B' is about 3 N/mm<sup>2</sup> larger than that of the area A'. In the area A', it was expected that the internal deterioration separated the surface mortar from the wall concrete. For this reason, it seems that the rebound value measured by Schmidt hammer became small. The internal state of structures affects the rebound value and thus Schmidt hammer could detect internal deterioration.

The rebound value of area C' was 37.95 with  $F_C=18.19$  N/mm<sup>2</sup>, which was much larger than those of the areas A' and B'. Therefore, it was found that the both areas A' and B' have internal deterioration and, in particular, it is remarkable in the area A'. However, the area B' was estimated sound from the thermal image. Thus, if the deterioration spreads in a wide area, the selection of comparison objects is very important to avoid wrong diagnosis.

The temperature distribution of a concrete surface is considered to be affected by wetness condition as well as heating condition. Figure 12 (a) shows the temperature distribution of the retaining wall in the rain at 14:00 on December 16, 2014. No natural heating (the sun) was given on the day and because the wall was wet by rain, the temperature distribution was rather uniform. The surface temperature of the upper part of the wall was lower probably due to the loss of vaporization heat. It is considered to be difficult to detect deteriorated parts from infrared thermography on rainy days.

Measurement was also conducted on the time after rain stopped and the sun light illuminated the wall, at 13:00 on November 27, 2014 (Fig. 12(b)). The deteriorated parts were clearly identified by this image because the deteriorated parts dried up faster than other parts due to trapped heat. But the wetness condition is considered to be another factor to determine the surface temperature. Thus the condition of measuring objects should be examined carefully before conducting infrared thermography.

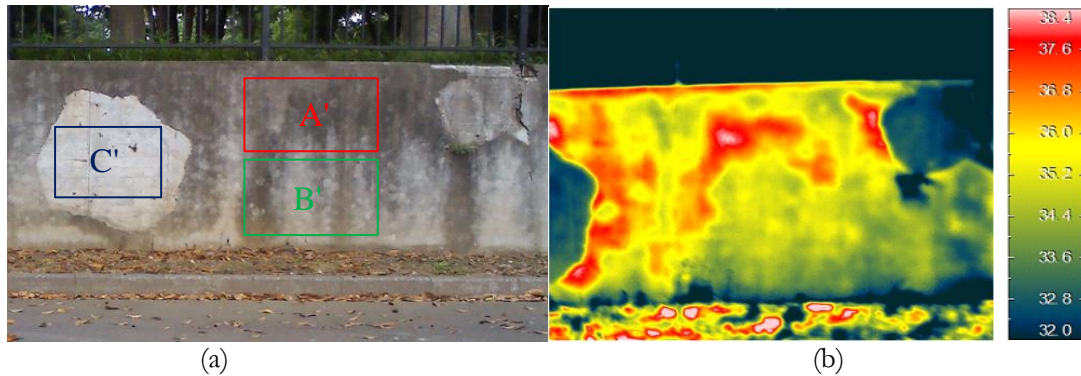


Fig. 11. (a) Measurement areas by Schmidt hammer on July 27, 2013; and (b) the corresponding thermal image.

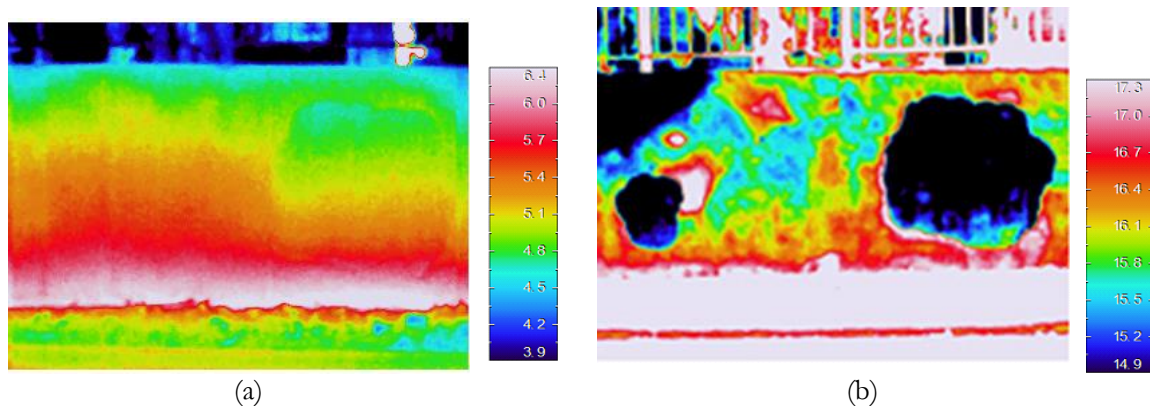


Fig. 12. (a) Thermal image measured in the rain at 14:00 on December 16, 2014; and (b) one just after rain stopped at 13:00 on November 27, 2014.

#### 4. Conclusions

In this study, basic measurements of deterioration for a concrete retaining wall were carried out by infrared thermography, rotary sounding hammer and Schmidt rebound hammer methods. In the deterioration evaluation by rotary hammer and thermography, the both diagnosis results were consistent. Thus, the deterioration diagnosis by infrared thermography is considered to be effective for concrete infrastructures. Rotary hammering test is an easy and simple diagnosis method but it cannot be used for a large extent of structures in a short time. Hence, infrared thermography is considered to be very effective to confirm the shape and size of internal deterioration quickly. In the deterioration evaluation by Schmidt hammer and thermography, two deteriorated areas were detected by Schmidt hammer but one of them was not detected by infrared thermography. From the rebound values by Schmidt hammer, it is considered that the both areas have internal deterioration and the retaining wall was deteriorated significantly as a whole.

The diagnosis by infrared thermography can detect deterioration from the temperature difference with respect to the surrounding areas. Therefore, the comparison areas have to be selected carefully to prevent overlooking deteriorated parts. To do this, thermal images of a healthy state of structures need to be captured before deterioration is in progress and it is considered that an accurate diagnosis is possible by comparing multi-temporal thermal images acquired at various air temperature and sun light conditions.

#### References

- [1] Japan Ministry of Land, Infrastructure and Transport, "White Paper on Land, Infrastructure and Transport in Japan 2015," 2016.
- [2] U.S. Department of Transportation, Federal Highway Administration, "2015 Status of the Nation's Highways, Bridges and Transit: Conditions and Performance," 2017.
- [3] S. Takahara, "Maintenance of Railway infrastructure. Countermeasures to deterioration of infrastructure on small- and mid-sized railways: Current status of railway infrastructure," *Japan Railway & Transport Review*, no. 62, pp. 40-48, 2013.

- [4] M. Kunishima and Y. Ishihara, "Concrete flaking in a Shinkansen tunnel of West Japan Railway Co.: June 27th, 1999 and October 9th, 1999, Fukuoka Prefecture," in *Failure Knowledge Database: 100 Selected Cases*. 1999.
- [5] M. S. Chalhoub, "Effect of reinforced concrete deterioration and damage on the seismic performance of structures," *Structural Nonlinear Dynamics and Diagnosis*, vol. 168, pp. 77-95, 2015.
- [6] Applied Technology Council, "FEMA 307 Evaluation of earthquake damaged concrete and masonry wall buildings concrete and masonry wall buildings," *Technical Resources*, 1998. Available: <https://mitigation.eeri.org/files/fema-306.pdf> [Accessed: 5 July 2017]
- [7] Y. Nakano, M. Maeda, H. Kuramoto, and M. Murakami, "Guideline for post-earthquake damage evaluation and rehabilitation of RC buildings in Japan," in *13th World Conference on Earthquake Engineering*, paper no. 124, 2004.
- [8] California Department of Transportation, "Visual inspection & capacity assessment of earthquake damaged reinforced concrete bridge elements," Report no. CA08-0284, 2008.
- [9] K. Kawashima and S. Unjoh, "The damage of highway bridges in the 1995 Hyogo-ken Nambu earthquakes and its impact on Japanese seismic design," *Journal of Earthquake Engineering*, vol. 1, no. 3, pp. 505-541, 1997.
- [10] F. Yamazaki, H. Motomura, and T. Hamada, "Damage assessment of expressway networks in Japan based on seismic monitoring," in *Proc. 12th World Conference on Earthquake Engineering*, 2000.
- [11] J. Helal, M. Sofi, and P. Mendis, "Non-destructive testing of concrete: A review of methods," *Electronic Journal of Structural Engineering*, vol. 14, no. 1 (special issue), 2015.
- [12] M. M. Lima, D. Miller, and J.-H. Doh, "Structural health monitoring of concrete bridges in Guilan Province based on a visual inspection method," *Structural Durability & Health Monitoring*, vol. 9, no. 4, pp. 269-285, 2013.
- [13] Y. Fujino and D. M. Siringoringo, "Bridge monitoring in Japan: the needs and strategies," *Structure and Infrastructure Engineering*, vol. 7, no. 7-8, pp. 597-611, 2011.
- [14] Y. Fujita, Y. Mitani, and Y. Hamamoto, "A method for crack detection on a concrete structure," in *Proc. 18th International Conference on Pattern Recognition*, vol. 3, pp.901-904, 2006.
- [15] T. Yamaguchi and S. Hashimoto, "Fast crack detection method for large-size concrete surface images using percolation-based image processing," *Machine Vision and Applications*, vol. 21, no. 5, pp. 797-809, 2010.
- [16] C. C. Cheng, T. M. Cheng, and C. H. Chiang, "Defect detection of concrete structures using both infrared thermography and elastic waves," *Automation in Construction*, vol. 18, no. 1, pp. 87-92, 2008.
- [17] D. G. Aggelis, E. Z. Kordatos, D. V. Soulioti, and T. E. Matikas, "Combined use of thermography and ultrasound for the characterization of subsurface cracks in concrete," *Construction and Building Materials*, vol. 24, no. 10, pp. 1888-1897, 2010.
- [18] D. M. McCann and M. C. Forde, "Review of NDT methods in the assessment of concrete and masonry structures," *NDT & E International*, vol. 34, no. 2, pp. 71-84, 2001.
- [19] F. Cerdeira, M. E. Vázquez, J. Collazo, and E. Granada, "Applicability of infrared thermography to the study of the behaviour of stone panels as building envelopes," *Energy and Buildings*, vol. 43, no. 8, pp. 1845-1851, 2011.
- [20] Nippon Avionics Co. Ltd., "Infrared thermal camera and industrial measuring instruments," 2017. Available: <http://www.avio.co.jp/english/products/infrared/index.html> [Accessed: 5 July 2017]
- [21] Dogyu Sangyo Co. Ltd., "Exterior wall testing device," 2017. Available: <http://www.dogyu.jp/product/test/> [Accessed: 5 July 2017]
- [22] Y. Sonoda and Y. Fukui, "A basic study on hammering tests of deteriorated concrete structures," presented at *35th Conference on Our World in Concrete & Structures*, 2010.
- [23] Fuji Bussan Co. Ltd., "Schmidt concrete test hammer type N and NR," 2017. Available: [http://sooki.co.jp/upload/surveying\\_items/51001\\_tori.pdf](http://sooki.co.jp/upload/surveying_items/51001_tori.pdf) [Accessed: 5 July 2017]
- [24] *Standard for Assessing Concrete Compressive Strength Based on Schmidt Hammer Testing*, (in Japanese) The Society of Materials Science, Japan, 1958. Available: <http://www.jsms.jp/book/shumit.htm> [Accessed: 5 July 2017]
- [25] P. L. Yeh and P. L. Liu, "Application of the wavelet transform and the enhanced Fourier spectrum in the impact echo test," *NDT & E International*, vol. 41, no. 5, pp. 382-394, 2008.